Full Title: **Dabigatran prevents lipopolysaccharide mediated apoptosis in zebrafish through a thrombin independent mechanism**

Annelore I. T. Fleischmann[1], William H. Woodhams[1], Ritta Mouayed[1], Timmy Joseph[2], Xiangyu Sui[4], Murat Yaman[2], Stefan Oehlers[4], Jordan A. Shavit[2,3*], Vinitha A. Jacob[1*]

[1]Department of Emergency Medicine, University of Michigan Medical School, Ann Arbor, MI.

[2]Department of Pediatrics, University of Michigan Medical School, Ann Arbor, MI.

[3]Department of Human Genetics, University of Michigan Medical School, Ann Arbor, MI.

[4]A*STAR Infectious Diseases Labs (A*STAR ID Labs), Agency for Science, Technology and Research (A*STAR), Singapore, Singapore.

[*]Co-senior author

Corresponding author contact information:

Vinitha A. Jacob, MD, PhD

Department of Emergency Medicine

Taubman Center B1-220

1500 E. Medical Center Dr.

Ann Arbor, MI 48109-5301

Email: vijacob@umich.edu

Phone: 734-615-8232

Fax: 734-936-9414

Running Head: Dabigatran prevents lipopolysaccharide toxicity

The authors were supported in part by National Institutes of Health grants R35HL150784, K12HL133304 and K08GM151392.

Abstract: Endotoxemia is a feature of sepsis pathogenesis and has also been found to mediate the pathophysiology of multiple inflammatory conditions. In this work, we use a lipopolysaccharide (LPS) induced endotoxemia model in zebrafish to identify novel mediators of LPS toxicity. We performed transcriptomic studies on LPS-treated larvae, followed by *in silico* analysis, which revealed associations between the signatures of LPS-treated embryos and those of drugs involving diverse pathways. In parallel, we performed an *in vivo* screen using >1,500 FDA-approved compounds and identified multiple novel small molecules that reduced inflammation and prevented LPS toxicity. We focused on the direct thrombin inhibitor dabigatran, which was identified through both the *in vivo* and *in silico* analyses. We found that dabigatran co-administration significantly reduced the expression of inflammatory cytokines and completely protected zebrafish from endotoxemic death due to LPS. Surprisingly, we found that this protection occurs in prothrombin mutant fish, proving that protection from endotoxemia occurs independently of the anticoagulant function of dabigatran. We additionally found that dabigatran administration significantly decreased nitric oxide production and apoptosis compared to LPS treatment alone, suggesting possible mechanisms by which protection from endotoxemia is achieved. In summary, we identify several novel small molecules that prevent LPS-induced endotoxemia and show that one such small molecule, dabigatran, exerts a thrombin-independent effect on nitric oxide production and apoptosis. This and the other identified small molecules warrant further exploration in inflammatory conditions including sepsis.

Key Words: sepsis, small molecule screen, anticoagulant, thrombin, nitric oxide, inflammation, apoptosis

53 **Introduction:**

54 Lipopolysaccharide (LPS), a cell wall component of gram-negative bacteria, induces an immune
55 response upon recognition by Toll-Like Receptors (TLRs) [1,2]. LPS accounts for the relative
56 impermeability of the outer membrane of gram-negative bacteria to hydrophobic molecules, making them
57 resistant to many antimicrobials [3,4]. LPS-mediated endotoxemia mimics many features of sepsis
58 pathogenesis and might also play a causative role in the pathophysiology of multiple chronic
59 inflammatory disorders, including Parkinsons, Alzheimers, obesity, and atherosclerosis [5]. Previous work
60 in mammals suggests that the translocation of gut-derived LPS into the circulation might mediate some of
61 these disease states [6,7]. Additionally, LPS contributes to disease pathogenesis through its action as a
62 prothrombotic molecule; LPS-induced inflammatory mediators activate procoagulant pathways, induce
63 platelet activation, downregulate anticoagulant pathways and promote disseminated intravascular
64 coagulation [8,9]. Moreover, macrophages undergoing pyroptosis release tissue factor, further activating the
65 coagulation cascade [5,9].

66 Given its role in multiple diseases, efforts have been made to block LPS biogenesis, neutralize
67 endotoxin, and hinder LPS-mediated immune activation [10-13], with many of these attempts made in the
68 context of sepsis. However, there is the possibility that therapeutics targeting LPS signaling can also
69 mitigate the development of chronic inflammatory conditions such as those listed above.

70 In this work, we undertook large-scale *in silico* and *in vivo* analyses to identify novel small
71 molecule mediators of LPS toxicity. Murine and other mammalian models are cost-prohibitive for the
72 same types of large-scale *in vivo* screening studies. Zebrafish, on the other hand, allow for a speed of
73 discovery not possible with mammals as they combine the scalability of *in vitro* systems with the
74 complexity of a whole vertebrate organism.

75 In zebrafish, LPS-induced inflammation has been provoked either by injection into the embryonic
76 yolk sac or immersion of embryos and larvae into LPS-containing media [14-16]. Incubation with LPS-
77 containing media allows uniform, rapid treatment of large numbers of fish. A response remarkably similar

78 to that in mammals is observed, including inflammation, platelet activation, vascular leakage, and organ
79 damage [16]. Thus, many of the cardinal features of sepsis pathogenesis are recapitulated by this model.
80 We performed novel high throughput studies in a zebrafish model of LPS-provoked endotoxemia
81 with the goal of identifying drugs that could be repurposed to combat acute and chronic inflammatory
82 conditions. We conducted an *in silico* analysis, where we compared RNA-seq data from LPS-treated fish
83 to publicly available RNA-seq datasets, revealing associations between LPS and drugs involving
84 disparate pathways. In parallel, an *in vivo* pathway analysis was performed using >1,500 FDA-approved
85 compounds to find those that mitigated LPS-induced endotoxemia, uncovering multiple novel small
86 molecules. We focused on the sole anticoagulant (dabigatran) identified in both the *in silico* and *in vivo*
87 analyses. Interestingly, the administration of dabigatran reduced the upregulation of inflammatory
88 cytokines, significantly reduced nitric oxide production and apoptosis and abolished larval mortality from
89 endotoxemia due to LPS. Surprisingly, this protection was found to occur independent of its inhibitory
90 effect on thrombin. These data implicate dabigatran and other novel small molecules as anti-inflammatory
91 agents that can be explored as potential therapeutics in acute and chronic conditions.
92
93 **Materials and Methods:**
94 ***Animal care and husbandry:***
95 Zebrafish (*Danio rerio*) were raised in accordance with animal care guidelines as approved by the
96 University of Michigan Animal Care and Use Committee. Wild-type fish were a hybrid line generated by
97 crossing AB and TL strain zebrafish acquired from the Zebrafish International Resource Center. Genetic
98 knockouts of prothrombin (*f2*) have been previously described [17]. Tricaine (Western Chemical) was used
99 for anesthesia and rapid chilling in an ice water bath for euthanasia.
100
101 ***Small molecule treatments:***
102 Small molecule screens (MedChemExpress FDA drug repurposing set) were started at 3 dpf, where 3
103 larvae were plated per well in 96-well plates containing embryo media. All drugs were initially tested at a

concentration of 25 μM for resistance to LPS toxicity, and confirmatory studies were performed with a larger group of fish (9-45) representing at least three different clutches (3 separate experiments), where the drugs were tested at various concentrations.

Heart rate measurements:

Heart rate was measured 3 hours after lethal LPS (40 μg/mL) administration and compared to untreated controls. Larvae were mounted in 0.8% low melting point agarose and visualized using an Olympus IX73 microscope. Heart rate was manually counted over 60 seconds for each larva. Each experiment consisted of at least 15 larvae. At least three different clutches (3 different experiments) were utilized.

Real-time quantitative polymerase chain reaction (RT-qPCR):

RT-qPCR was performed as described previously [18]. Total RNA was extracted from 3 dpf whole larvae 3 hours post treatment using the RNeasy Mini Plus kit (Qiagen) and transcribed into cDNA using Superscript III cDNA synthesis kit (Invitrogen). Transcript levels of genes of interest were quantified by qPCR (Mastercycler realplex^2, Eppendorf) using Fast SYBR Green Mix (Applied Biosystems, Waltham, MA). Three equal pools of whole larvae (15-45 embryos per pool) were tested. Primer sequences are provided in Table S3. All expression data were normalized to the *actb2* gene, and significance was analyzed using the double delta C_t method as described [19].

RNA-seq preparation and analysis:

RNA-seq was performed as described previously [18]. Three biological replicate pools of 30-45 3 dpf whole embryos were used per condition. Total RNA was extracted, and cDNA was prepared as above. Samples were sent to Novogene (Sacramento, CA) for further processing. Paired-end 150 base pair (bp) sequencing was obtained with the Illumina NovaSeq 6000 Sequencing System. Reads were mapped to exonic regions based on the zebrafish reference genome (GRCz11) using STAR36 (v.2.7.9a) and

129 featureCounts37 (v.2.0.3). Differential expression analysis was conducted using the R package DESeq2
130 ([20]. All significant differentially expressed genes (FDR adjusted p-values) were converted to human genes
131 using the R package babelgene. KEGG Pathway Analysis was then performed using the Enrichr platform,
132 a publicly available tool [21,22]. Overlap score is the number of significantly changed genes over the total
133 number of genes in the pathway. The combined score considers the z-score (a value's relationship to the
134 mean) in addition to the adjusted p-value; this score has been found to outperform other ranking metrics
135 [22]. The combined score is used to assess the significance of gene set enrichment findings, with higher
136 values being more significant; values > 30 have been considered significant in literature [23,24].
137
138 ***Laser-mediated vascular endothelial injury:***
139 Larvae were treated with LPS and drug starting at 3 dpf and collected after 3 hours for assessment of time
140 to clot formation, performed as previously described [17,23,25,26]. Briefly, 3 dpf larvae were mounted in 0.8%
141 low melting point agarose and visualized using an Olympus IX73 microscope with an attached
142 Micropoint focusing system and pulsed-dye laser (Andor). For venous laser injury, 99 laser pulses were
143 administered to the ventral surface of the posterior cardinal vein, 5 somites caudal to the anal pore. For
144 arterial laser injury, 99 laser pulses were administered 5 somites caudal to the anal pore on the dorsal
145 surface of the dorsal aorta. Time to occlusion (formation of an occlusive thrombus) was measured, where
146 120 seconds was the maximum time each larva was observed. Three biological replicates were performed
147 for each experiment.
148
149 ***In silico analysis:***
150 Differential gene expression data were retrieved from the RNAseq results as previously described [18]. The
151 human orthologues of the respective genes were obtained from the Zebrafish Information Network
152 database (https://zfin.org/downloads/archive/2023.04.26) and the CLUE software platform was utilized in
153 performing Connectivity Map-based analyses
154 (https://www.sciencedirect.com/science/article/pii/S0092867417313090 (access date April 26, 2023)).

155 Genes were ranked based on the adjusted p-values for the gene expression level changes, and the top 150
156 upregulated or down-regulated genes were tested for the gene connectivity evaluations across 64 human
157 cell lines and disparate perturbation profiles. The connectivity data were processed by using cmapR
158 library in R (v4.2.2) environment (Natoli T (2023). cmapR: Cmap Tools in R. R package version
159 1.12.0, https://github.com/cmap/cmapR). The data were further filtered down to 27 cell lines of which
160 most were hematopoietic/hepatic/pulmonary/non-tumorigenic origins, or endothelial phenotypes (A375,
161 A549, ASC, BJAB, CD34, HA1E, HCC515, HEK293, HELA, HEPG2, HPTEC, HUH7, HUVEC,
162 JURKAT, K562, MCF10A, NCIH508, NCIH596, NOMO1, OCILY19, OCILY3, PHH, THP1, TMD8,
163 U2OS, U937, YAPC).
164
165 ***Acridine Orange Staining:***
166 Larvae were incubated in 10 µg/ml Acridine Orange stain (Sigma) for 15 minutes in embryo media
167 with LPS treatment and then rinsed three times before mounting in 0.8% agarose and imaged with an
168 Olympus IX73 microscope. Quantification of intensity was performed in ImageJ.
169
170 ***TUNEL Staining:***
171 The TUNEL assay was performed according to the instructions provided in the In Situ Cell Death
172 Detection Kit, TMR red (Roche) for cryopreserved samples, with embryos cryopreserved in Optimal
173 Cutting Temperature Compound (OCT) and cryosectioned prior to labeling. Images were quantified by
174 an observer blinded to condition using a visual scoring system. The visual scoring system consisted of
175 grades 0 through 3 (0 = 0-9% fluorescence in visual field, 1 = 10-20% fluorescence, 2 = 30-70%
176 fluorescence, 3 = 80-100% fluorescence).
177
178
179

180 ***NO Staining:***

181 Larvae were split into four treatment groups: control, LPS, dabigatran, and LPS with dabigatran. Each
182 treatment group was simultaneously incubated with 5 uM of DAF-FM-DA solution in the dark at 25°C as
183 previously described (Lepiller et al., 2007). After 2 hours larvae were washed with embryo media and
184 mounted in 0.8% agarose. Imaging was done using an Olympus IX73 microscope. Fluorescence
185 quantification was obtained utilizing ImageJ.

186

187 ***Tail transection:***

188 Tg(lyzC:GFP)^{nz117} and TgBAC(mpeg1.1:EGFP)^{vcc7} transgenic larvae were anesthetized at 5 days post
189 fertilization and tail transection was performed with a sterile scalpel blade. Wounded larvae were
190 transferred into fresh embryo media with 25 µM dabigatran and incubated at 28.5 °C for 5 hours
191 prior to imaging using a Nikon SMZ25 stereoscope. Leukocyte recruitment was quantified by measuring
192 the fluorescent pixel area within 100 µm of the wound site in FIJI/ImageJ.

193

194 ***Statistics:***

195 Statistics were performed using the GraphPad PRISM package. $P<0.05$ was considered significant. For
196 qPCR and RNA-seq data, Student's t-test on $\Delta\Delta C_t$ values was used to determine significance. For time to
197 occlusion (TTO) data, Mann-Whitney *U* testing was used to determine significance.

198

199 ***Study Approval:***

200 Approval for zebrafish studies was granted by the University of Michigan Institutional Animal Care and
201 Use Committee, identification number PRO00010679 and the A*STAR Institutional Animal Care and
202 Use Committee, identification numbers 211667 and 221694.

203

204

205 **Results:**

206 ***LPS incubation results in inflammatory and coagulopathic changes in zebrafish embryos***

207 *S. typhi* LPS was administered to zebrafish by incubation starting at 3 days post fertilization (dpf)
208 in accordance with published data [16]. A dose-dependent effect on lethality was noted over 24 hours.
209 Hereafter, the lethal dose of LPS refers to the smallest amount that caused uniform lethality by 4 dpf,
210 which was slightly different (ranging from 40-50 μg/mL) depending on the batch. A new dose-response
211 curve was made for each batch of LPS tested, and an example is shown in Fig. 1A. In addition to
212 increased mortality, heart rate was significantly decreased (Fig. 1B), and *grk5,* a gene involved in heart
213 contractility, was significantly downregulated 3 hours after LPS administration (Fig. 1C).

214 To determine the significant biological pathways altered upon LPS administration, RNA-seq was
215 performed on treated fish compared to controls as previously described (Guirgis et al., 2023). Kyoto
216 Encyclopedia of Genes and Genomes (KEGG) pathway analysis was performed and revealed that
217 "Pathogenic *E. coli* Infection" was the most significantly altered pathway in LPS-treated fish (Fig. 2A,
218 complete analysis is shown in Table S1), confirming that administration induces a response akin to that
219 provoked by bacteria. As expected, immune and interferon pathways such as TNF signaling were
220 significantly changed (Fig. 2A). A subset of genes from these pathways were confirmed by qPCR and
221 trended toward upregulation, with the genes *il1b*, *il6* and *irg1l* significantly upregulated (Fig. 2B). In
222 addition to provoking a proinflammatory response, LPS is also known to be a prothrombotic molecule [7,9].
223 RNA-seq data also showed that the complement, coagulation, and platelet activation pathways were
224 significantly altered in LPS-treated zebrafish compared to controls (Fig. 2A). A subset of procoagulant
225 genes from these pathways was upregulated, which was confirmed by qPCR (Fig. 2B). Interestingly,
226 tissue factor b (gene *f3b*), but not tissue factor a (gene *f3a*) was significantly upregulated in LPS-treated
227 fish compared to controls, suggesting possible arterial injury as *f3b* is thought to play a primary role in
228 arterial, rather than venous, circulation [26]. Time to occlusion (TTO) after venous and arterial laser-
229 mediated endothelial injury was measured as previously described [23,26] and is illustrated in Fig. 2D. The

230 TTO was found to be significantly increased in fish administered LPS for both systems (Fig. 2E, F). This
231 change suggests a consumptive coagulopathy phenotype similar to what we have observed with the loss
232 of natural anticoagulants [23,27].
233
234 ***In silico and in vivo analysis reveals small molecule mediators of LPS-mediated endotoxemia***
235 To identify possible mediators of LPS toxicity, we initially undertook an *in silico* analysis
236 comparing the RNA-seq signature of LPS-treated embryos to those of genes and compounds from
237 publicly available databases (Table S2). After obtaining the list of small molecules related to LPS based
238 on the gene expression profiles (Table S2), we further looked into mechanisms of action for each of these
239 unique molecules as provided by the Connectivity Map (CMap) database. Even though some compounds
240 did not have an annotated MoA, the data showed an intriguing pattern among the ones with detailed
241 annotations. Notably, neuroactive compounds such as dopamine and serotonin receptor antagonists, along
242 with ion channel and kinase inhibitors, emerged as the most commonly shared classes amongst the LPS-
243 associated compounds (Table 1).
244 In parallel, we performed an *in vivo* analysis in zebrafish embryos. A lethal dose of LPS was co-
245 administered at 3 dpf with an FDA-approved drug repurposing set consisting of >1500 compounds.
246 Embryos were examined for survival 24 hours post-treatment, and each drug that was a 'hit' (i.e., enabled
247 survival of at least one embryo) was validated in a larger cohort to confirm rescue. Approximately 20
248 small molecules were identified in this manner (Table 2). Most hits completely protected against LPS
249 toxicity during the embryonic/early larval period, and others provided partial protection (Table 2, Fig. S1
250 A-T). These small molecule mediators of LPS toxicity spanned multiple categories, most heavily
251 represented by serotonin and dopamine receptor modulators, chemotherapeutics, and anti-infectious
252 agents. Similar to the *in silico* analysis, small molecules modulating the dopamine and serotonin
253 pathways and those affecting tyrosine kinases were heavily represented *in vivo*. Four drugs were hits in
254 both the *in silico* and *in vivo* analyses; these were amsacrine, conivaptan, vilazodone and dabigatran

255 etexilate (the prodrug formulation of dabigatran, hereafter referred to simply as dabigatran) (Table S2,
256 Table 2). Approximately half of the drugs identified *in vivo* (berberine, ketanserin, sunitinib, ceritinib,
257 fedratinib, nelfinavir, saquinavir, indacaterol, dabigatran) have been shown to ameliorate LPS effects, and
258 to function as mammalian anti-sepsis agents [28-48], suggesting conservation between zebrafish and
259 mammals in terms of the effects of these small molecules. The remaining hits from the *in vivo* screen –
260 ziprasidone, pergolide, vilazodone, bedaquiline, rucaparib, pralsetinib, amsacrine, conivaptan,
261 deserpidine, and lomitapide – are, to our knowledge, novel mediators of LPS toxicity (Table 2). Despite
262 some variability, there was an overall trend toward decreased inflammatory cytokine production when a
263 subset of these drugs were co-administered with LPS and compared to LPS treatment alone (Fig. S2 A-
264 L). Thus, these novel mediators of LPS toxicity may function as anti-inflammatory agents.
265
266 ***Dabigatran reduces LPS mediated inflammation and mortality***
267 Given the availability of tools to study coagulation in zebrafish [25,49] we decided to characterize further the
268 one anticoagulant, dabigatran, that was identified through both *in silico* and *in vivo* analyses. Although a
269 prior study has shown only a modest effect of dabigatran on lethality in sepsis models [39], we found that it
270 completely averted LPS-induced lethality (Fig. 3A). Expression of inflammatory cytokines and
271 procoagulant genes were downregulated in fish co-treated with LPS and dabigatran compared to LPS
272 alone (Fig. 3B). As previously shown [17], time to venous occlusion was increased in dabigatran treated
273 fish, indicating successful anticoagulation (Fig. 3C). There was no additive effect on occlusion with co-
274 treatment.
275 We next determined whether dabigatran administration could produce a more general anti-
276 inflammatory effect. Tail transection, an established method to induce inflammation, was performed on 3
277 dpf larvae. We found that dabigatran did not reduce neutrophil or macrophage recruitment to the tail
278 transection site, suggesting that its protection might be more specific to LPS rather than representing a
279 general anti-inflammatory response (Fig. S3).
280

281 ***Dabigatran protects zebrafish from LPS toxicity independent of its anticoagulant function***

282 An anti-sepsis effect of dabigatran mediated through fibrinogen-like protein 2 (Fgl2) has been described
283 [39]. To determine whether the protection from LPS toxicity was dependent on the anticoagulant effect of
284 dabigatran, we evaluated three other commonly used anticoagulants – two affecting factor Xa,
285 rivaroxaban and apixaban, as well as another thrombin inhibitor, argatroban. Rivaroxaban and apixaban
286 were previously shown to be active in zebrafish and were used here at the same concentration [17].
287 However, we required shorter incubation times due to the rapid lethality induced by LPS. As expected, all
288 anticoagulants increased the TTO (Fig. 4A, Fig. S4 A, B). Interestingly, some of the anticoagulants
289 appeared to have a synergistic effect with LPS, significantly increasing the time to occlusion when
290 compared to the drug alone (Fig. 4A, Fig. S4 A, B). However, none of these conferred protection from
291 LPS toxicity (Fig. 4B, Fig. S4 C, D), suggesting that anticoagulation might not be the mechanism through
292 which dabigatran mitigates LPS-induced endotoxemia.

293 To further test this hypothesis, we employed a prothrombin knockout background (null mutation
294 in the *f2* gene [17]. Larvae from *f2* heterozygous incrosses were divided into four groups: untreated controls,
295 LPS, dabigatran, and LPS + dabigatran. Each group was followed for survival over 3 days. LPS alone was
296 lethal in all genotypes (Fig. 4C), revealing that thrombin inhibition is not necessary for protection from
297 LPS. The presence of homozygous mutants was confirmed by genotyping all clutches, except for LPS
298 alone due to their rapid degradation (Fig. 4D). Thus, dabigatran administration protected *f2* homozygous
299 mutants from lethal LPS, proving that its mechanism of protection occurs independently of thrombin
300 inhibition.

301

302 ***Dabigatran administration reduces LPS mediated nitric oxide production and apoptosis***

303 Nitric oxide (NO) production can contribute to the hypotension seen in septic shock [50], and LPS has
304 previously been showed to increase NO [50]. We confirmed that LPS administration increased NO
305 production in our system (Fig. 5A, B). Additionally, dabigatran has previously been found to suppress

306 nitric oxide synthase [51]. We therefore tested whether dabigatran treatment could reduce NO production
307 and found this to be the case (Fig. 5A, B).
308 RNA sequencing data suggested that apoptosis related pathways were increased in LPS-treated
309 fish (Fig. 6A). As NO production has been shown to lead to apoptosis after LPS exposure [52], we next
310 tested whether this represented a mechanism by which protection from LPS is conferred. We found that
311 cell death (Fig. 6B, C) and apoptosis (Fig. 6D, E) were significantly decreased in dabigatran and LPS co-
312 treated fish. These data suggest that decreased NO production and apoptosis might be mechanisms by
313 which dabigatran protects against LPS toxicity.
314
315 **Discussion:**
316 We have identified several small molecule mediators of LPS toxicity that can act as anti-
317 inflammatory agents. Approximately half had been previously explored in mammalian LPS models, and
318 all have been shown to reduce inflammation and ameliorate toxicity [28-31,33-37,40,42,43,47,48,53-55], suggesting
319 strong concordance between zebrafish and mammals. These mediators were found to act through multiple
320 mechanisms, including inhibition of TLR and NFκB activation [33,54] as well as inhibition of inflammation
321 through NFκB-independent mechanisms [34,35]. Other potential mechanisms include effects on apoptosis [30]
322 and NOS (nitric oxide synthase) activation [31]. A smaller number of the identified drugs have also been
323 investigated in mammalian sepsis models [32,39,41,43-45,47,56], all with beneficial effects, indicating further
324 concordance with our zebrafish data. The novel mediators of LPS toxicity that have not previously been
325 tested in other studies – amsacrine, bedaquiline, conivaptan, deserpidine, lomitapide, pergolide,
326 prasetinib, rucaparib, vilazodone, ziprasidone – have as yet undetermined mechanisms of action and
327 represent avenues for further research in both mammalian inflammation and sepsis.
328 Clinical trials using anticoagulants in the context of sepsis have proven equivocal at best [57-66],
329 although it is still possible that specific subtypes of sepsis patients may benefit from anticoagulant
330 therapy. Previous studies have shown that dabigatran reduces inflammation ([39,40] and can enhance survival

331 in mouse models of sepsis [39], congruent with a cohort study revealing that patients on dabigatran had a
332 lower incidence of *Staphylococcus aureus* bacteremia [41]. Dabigatran has also been found to mitigate
333 inflammation in multiple contexts, including diet [67], oxysterols [68], and acute myocardial infarction [51].
334 However, it is unclear whether these beneficial effects were due to the anticoagulant function of
335 dabigatran. Our data suggest that dabigatran reduces inflammation and promotes survival from LPS
336 toxicity through a novel mechanism independent of its direct anticoagulant effect on thrombin.
337 We found that dabigatran administration reduces LPS mediated NO production and apoptosis,
338 suggesting that this is one possible mechanism by which dabigatran confers protection from LPS.
339 Dabigatran has previously been shown to suppress nitric oxide synthase in acute myocardial infarction [51]
340 and future experiments will clarify the mechanism by which dabigatran reduces LPS mediated nitric
341 oxide production.
342 There are several limitations of this study. Due to the stringency of the screen (mortality), it is
343 likely that other small molecules conferring beneficial effects but not affecting mortality (e.g., those that
344 reduce inflammation) were not identified. This study also does not necessarily identify the mechanism by
345 which each drug acts to reduce LPS toxicity. It is possible that the effect is mediated through a non-
346 primary or previously unknown mechanism of action (as is the case with dabigatran).
347 Our data suggest that the novel small molecule mediators of LPS toxicity uncovered through our
348 screen can be explored as anti-inflammatory and anti-sepsis agents in mammals. Given that the hits
349 previously examined in mammalian systems were also found to have beneficial effects in this zebrafish
350 model, we expect that at least some of the novel drugs will translate to mammalian models.
351 Previous work and our data suggest that dabigatran can act as an anti-inflammatory and potential
352 anti-sepsis agent [39-41]. We show here definitive proof that dabigatran acts independently of thrombin to
353 exert its rescue of lethal endotoxemia. Venous thromboembolism prophylaxis is the standard of care for
354 most adult hospitalized inpatients, especially those admitted for sepsis [69,70]. The most common agents
355 used are unfractionated and low molecular weight heparins, but the data from our study suggest the
356 possibility that dabigatran could be an alternative with a dual benefit –both anticoagulant and completely

357 distinct anti-LPS functions. Randomized controlled trials in human inflammatory conditions or inpatients
358 would be relatively easy to support given the successful use of direct oral anticoagulants and the
359 indication for anticoagulation in hospitalized patients [69,70].
360
361
362
363 **Acknowledgments:**
364 A*STAR IMCB Aquarium Platform for expert zebrafish husbandry.
365
366 **Competing Interests:**
367 J.A.S. has been a consultant for Sanofi, Takeda, Genentech, CSL Behring, Pfizer, Medexus and
368 NovoNordisk. The other authors declare that they have no competing interests to disclose
369
370 **Funding:**
371 The authors were supported by the National Institutes of Health (https://www.nih.gov/) [R35HL150784
372 (J.A.S.), K12HL133304 and K08GM151392 (V.J.) and the Charles Woodson Collaborative Research
373 Award (J.A.S and V.J.)], the Singapore National Medical Research Council (https://www.nmrc.sg/
374)[OFIRG22jul-0081 (S.H.O.)]. J.A.S. is the Henry and Mala Dorfman Family Professor of Pediatric
375 Hematology/Oncology. X.S. holds the A*STAR Singapore International Graduate Award (SINGA)
376 scholarship (https://www.a-star.edu.sg/Scholarships/for-graduate-studies/singapore-international-
377 graduate-award-singa).
378
379 The funders had no role in study design, data collection and analysis, decision to publish, or preparation
380 of the manuscript.
381

382 **Data Availability:**

383 RNAseq data have been submitted to NCBI Gene Expression Omnibus and are available under accession
384 number GSE245299. Any other original data can be obtained by contacting the corresponding author at
385 vijacob@umich.edu.

386

387

388 **Author Contributions:**

389 V.J., J.A.S., S.O. and A.F. conceived and planned experiments. V.J., A.F., R.M., W.W. and X.S.
390 performed and analyzed all experiments and M.Y. performed *in silico* analysis. V.J. wrote the manuscript,
391 with input from all authors. J.A.S. revised the manuscript.

392

393

394

395

396

397

398

399

400

401

402

403

404

405

406

References:

1. Lewis AJ, Seymour CW, Rosengart MR. Current murine models of sepsis. *Surgical infections*. 2016;17(4):385-393.
2. Opal SM. Endotoxins and other sepsis triggers. *Contrib Nephrol*. 2010;167(167):14-24.
3. Nikaido H. Molecular basis of bacterial outer membrane permeability revisited. *Microbiology and molecular biology reviews*. 2003;67(4):593-656.
4. Bertani B, Ruiz N. Function and biogenesis of lipopolysaccharides. *EcoSal Plus*. 2018;8(1):10.1128/ecosalplus. ESP-0001-2018.
5. Page MJ, Kell DB, Pretorius E. The role of lipopolysaccharide-induced cell signalling in chronic inflammation. *Chronic Stress*. 2022;6:24705470221076390.
6. Violi F, Cammisotto V, Bartimoccia S, Pignatelli P, Carnevale R, Nocella C. Gut-derived low-grade endotoxaemia, atherothrombosis and cardiovascular disease. *Nature Reviews Cardiology*. 2022:1-14.
7. Violi F, Pignatelli P, Castellani V, Carnevale R, Cammisotto V. Gut dysbiosis, endotoxemia and clotting activation: A dangerous trio for portal vein thrombosis in cirrhosis. *Blood Reviews*. 2022:100998.
8. Yang X, Cheng X, Tang Y, et al. Bacterial endotoxin activates the coagulation cascade through gasdermin D-dependent phosphatidylserine exposure. *Immunity*. 2019;51(6):983-996. e6.
9. Wu C, Lu W, Zhang Y, et al. Inflammasome activation triggers blood clotting and host death through pyroptosis. *Immunity*. 2019;50(6):1401-1411. e4.
10. Warren HS, Danner RL, Munford RS. Anti-endotoxin monoclonal antibodies. Mass Medical Soc; 1992. p. 1153-1157.
11. Fisher Jr CJ, Slotman GJ, Opal SM, et al. Initial evaluation of human recombinant interleukin-1 receptor antagonist in the treatment of sepsis syndrome: a randomized, open-label, placebocontrolled multicenter trial. *Critical care medicine*. 1994;22(1):12-21.
12. Srinivas N, Jetter P, Ueberbacher BJ, et al. Peptidomimetic antibiotics target outer-membrane biogenesis in Pseudomonas aeruginosa. *Science*. 2010;327(5968):1010-1013.
13. Sperandeo P, Martorana AM, Polissi A. Lipopolysaccharide biogenesis and transport at the outer membrane of Gram-negative bacteria. *Biochimica et Biophysica Acta (BBA)-Molecular and Cell Biology of Lipids*. 2017;1862(11):1451-1460.
14. Yang L-L, Wang G-Q, Yang L-M, Huang Z-B, Zhang W-Q, Yu L-Z. Endotoxin molecule lipopolysaccharide-induced zebrafish inflammation model: a novel screening method for anti-inflammatory drugs. *Molecules*. 2014;19(2):2390-2409.
15. Yang L, Zhou X, Huang W, et al. Protective effect of phillyrin on lethal LPS-induced neutrophil inflammation in zebrafish. *Cellular Physiology and Biochemistry*. 2018;43(5):2074-2087.
16. Philip AM, Wang Y, Mauro A, et al. Development of a zebrafish sepsis model for high-throughput drug discovery. *Molecular Medicine*. 2017;23:134-148.
17. Grzegorski SJ, Hu Z, Liu Y, et al. Disruption of the kringle 1 domain of prothrombin leads to late onset mortality in zebrafish. *Scientific reports*. 2020;10(1):4049.
18. Guirgis FW, Jacob V, Wu D, et al. DHCR7 Expression Predicts Porsusor Outcomes and Mortality From Sepsis. *Critical Care Explorations*. 2023;5(6)
19. Schmittgen TD, Livak KJ. Analyzing real-time PCR data by the comparative CT method. *Nature protocols*. 2008;3(6):1101-1108.
20. Love MI, Huber W, Anders S. Moderated estimation of fold change and dispersion for RNA-seq data with DESeq2. *Genome biology*. 2014;15(12):1-21.

21. Chen EY, Tan CM, Kou Y, et al. Enrichr: interactive and collaborative HTML5 gene list enrichment analysis tool. *BMC bioinformatics*. 2013;14(1):1-14.
22. Kuleshov MV, Jones MR, Rouillard AD, et al. Enrichr: a comprehensive gene set enrichment analysis web server 2016 update. *Nucleic acids research*. 2016;44(W1):W90-W97.
23. Liu Y, Kretz CA, Maeder ML, et al. Targeted mutagenesis of zebrafish antithrombin III triggers disseminated intravascular coagulation and thrombosis, revealing insight into function. *Blood, The Journal of the American Society of Hematology*. 2014;124(1):142-150.
24. Zachariou M, Minadakis G, Oulas A, Afxenti S, Spyrou GM. Integrating multi-source information on a single network to detect disease-related clusters of molecular mechanisms. *Journal of proteomics*. 2018;188:15-29.
25. Rost M, Grzegorski S, Shavit J. Quantitative methods for studying hemostasis in zebrafish larvae. *Methods in cell biology*. Elsevier; 2016:377-389.
26. Grzegorski SJ, Zhao Y, Richter CE, et al. Genetic duplication of tissue factor reveals subfunctionalization in venous and arterial hemostasis. *PLoS Genetics*. 2022;18(11):e1010534.
27. Ku C-J, Yu X, Zhao QY, et al. Loss of protein C vs protein S results in discrepant thrombotic phenotypes. *Blood Advances*. 2025;9(3):545-557.
28. Zhang G, Zhang X, Huang H, Ji Y, Li D, Jiang W. Saquinavir plus methylprednisolone ameliorates experimental acute lung injury. *Brazilian Journal of Medical and Biological Research*. 2018;51
29. Zhao Y, Liu P, Luan H, et al. Demethyleneberberine alleviated the inflammatory response by targeting MD-2 to inhibit the TLR4 signaling. *Frontiers in Immunology*. 2023;14:1130404.
30. Fu K, Chen H, Mei L, et al. Berberine enhances autophagic flux by activating the Nrf2 signaling pathway in bovine endometrial epithelial cells to resist LPS-induced apoptosis. *Animal Science Journal*. 2023;94(1):e13847.
31. Liu C, Zhang X, Zhou J-X, et al. The protective action of ketanserin against lipopolysaccharide-induced shock in mice is mediated by inhibiting inducible NO synthase expression via the MEK/ERK pathway. *Free Radical Biology and Medicine*. 2013;65:658-666.
32. Vellinga NA, Veenstra G, Scorcella C, et al. Effects of ketanserin on microcirculatory alterations in septic shock: An open-label pilot study. *Journal of critical care*. 2015;30(6):1156-1162.
33. Zhao S, Gao N, Qi H, et al. Suppressive effects of sunitinib on a TLR activation-induced cytokine storm. *European Journal of Pharmacology*. 2019;854:347-353.
34. Dayang E-Z, Luxen M, Kuiper T, et al. Pharmacological inhibition of focal adhesion kinase 1 (FAK1) and anaplastic lymphoma kinase (ALK) identified via kinome profile analysis attenuates lipopolysaccharide-induced endothelial inflammatory activation. *Biomedicine & Pharmacotherapy*. 2021;133:111073.
35. Wallet MA, Reist CM, Williams JC, et al. The HIV-1 protease inhibitor nelfinavir activates PP2 and inhibits MAPK signaling in macrophages: a pathway to reduce inflammation. *Journal of leukocyte biology*. 2012;92(4):795-805.
36. Maarsingh H, Oldenburger A, Han B, et al. Effects of (a Combination of) the Beta2-Adrenoceptor Agonist Indacaterol and the Muscarinic Receptor Antagonist Glycopyrrolate on Intrapulmonary Airway Constriction. *Cells*. 2021;10(5):1237.
37. Aritake H, Tamada T, Murakami K, et al. Effects of indacaterol on the LPS-evoked changes in fluid secretion rate and pH in swine tracheal membrane. *Pflügers Archiv-European Journal of Physiology*. 2021;473(6):883-896.

38. Gill SK, Marriott HM, Suvarna SK, Peachell PT. Evaluation of the anti-inflammatory effects of β-adrenoceptor agonists on human lung macrophages. *European journal of pharmacology*. 2016;793:49-55.
39. Lei J, Zhou Y, Zhao H, et al. Dabigatran activates inflammation resolution by promoting fibrinogen-like protein 2 shedding and RvD5n-3 DPA production. *Theranostics*. 2021;11(9):4251.
40. Kimura G, Takahashi R, Nagamoto A, et al. Inhibitory Effects of Dabigatran on Airway Inflammation Induced by Lipopolysaccharide in Mice. *Yakugaku Zasshi: Journal of the Pharmaceutical Society of Japan*. 2020;140(12):1477-1483.
41. Butt JH, Fosbøl EL, Verhamme P, et al. Dabigatran and the risk of Staphylococcus aureus bacteremia: a nationwide cohort study. *Clinical Infectious Diseases*. 2021;73(3):480-486.
42. Akcora BO, Dathathri E, Ortiz-Perez A, et al. TG101348, a selective JAK2 antagonist, ameliorates hepatic fibrogenesis in vivo. *FASEB Journal*. 2019;33(8):9466-9475.
43. Hu J, Zhang W, Liu Y, et al. LDK 378 inhibits the recruitment of myeloid-derived suppressor cells to spleen via the p38–GRK 2–CCR 2 pathway in mice with sepsis. *Immunology and Cell Biology*. 2019;97(10):902-915.
44. Chen L, Liu X, Wang X, Lu Z, Ye Y. Berberine Alleviates Acute Lung Injury in Septic Mice by Modulating Treg/Th17 Homeostasis and Downregulating NF-κB Signaling. *Drug Design, Development and Therapy*. 2023:1139-1151.
45. Asila A, Liu J, Liu J, Li L, Liao J. Immunomodulatory effects of berberine on Staphylococcus aureus-induced septic arthritis through down-regulation of Th17 and Treg signaling pathways. *Acta Biochimica Polonica*. 2022;69(1):215-226.
46. Li B, Niu S, Geng H, Yang C, Zhao C. Berberine attenuates neonatal sepsis in mice by inhibiting FOXA1 and NF-κB signal transduction via the induction of MiR-132-3p. *Inflammation*. 2021;44(6):2395-2406.
47. Tong Y, Yu Z, Chen Z, et al. The HIV protease inhibitor Saquinavir attenuates sepsis-induced acute lung injury and promotes M2 macrophage polarization via targeting matrix metalloproteinase-9. *Cell death & disease*. 2021;12(1):67.
48. Chen H, Liu Q, Liu X, Jin J. Berberine attenuates septic cardiomyopathy by inhibiting TLR4/NF-κB signalling in rats. *Pharmaceutical Biology*. 2021;59(1):119-126.
49. Raghunath A, Ferguson AC, Shavit JA. Fishing for answers to hemostatic and thrombotic disease: Genome editing in zebrafish. *Research and Practice in Thrombosis and Haemostasis*. 2022;6(5)
50. Kirkebøen K, Strand Ø. The role of nitric oxide in sepsis–an overview. *Acta Anaesthesiologica Scandinavica*. 1999;43(3):275-288.
51. Song K, Wang Y, Sheng J, Ma C, Li H. Effects of dabigatran regulates no-reflow phenomenon in acute myocardial infarction mice through anti-inflammatory and anti-oxidative activities and connective tissue growth factor expression. *Molecular Medicine Reports*. 2018;17(1):580-585.
52. Xaus J, Comalada M, Valledor AF, et al. LPS induces apoptosis in macrophages mostly through the autocrine production of TNF-α. *Blood, The Journal of the American Society of Hematology*. 2000;95(12):3823-3831.
53. Sugino H, Futamura T, Mitsumoto Y, Maeda K, Marunaka Y. Atypical antipsychotics suppress production of proinflammatory cytokines and up-regulate interleukin-10 in lipopolysaccharide-treated mice. *Progress in Neuro-Psychopharmacology and Biological Psychiatry*. 2009;33(2):303-307.

543 54. Yao K, Wang Z, Peng C, et al. HIV protease inhibitor Saquinavir inhibits toll-like receptor
544 4 activation by targeting receptor dimerization. *Immunopharmacology and Immunotoxicology*.
545 2023;(just-accepted):1-10.
546 55. Chen N, Wang X-C, Fan L-L, Zhu Y-H, Wang Q, Chen Y-B. Berberine ameliorates
547 lipopolysaccharide-induced cognitive impairment through SIRT1/NRF2/NF-κB signaling
548 pathway in C57BL/6J Mice. *Rejuvenation Research*. 2022;25(5):233-242.
549 56. Weaver JG, Rouse MS, Steckelberg JM, Badley AD. Improved survival in experimental
550 sepsis with an orally administered inhibitor of apoptosis. *The FASEB journal*. 2004;18(11):1185-
551 1191.
552 57. Fourrier F, Chopin C, Huart J-J, Runge I, Caron C, Goudemand J. Double-blind, placebo-
553 controlled trial of antithrombin III concentrates in septic shock with disseminated intravascular
554 coagulation. *Chest*. 1993;104(3):882-888.
555 58. Diaz-Cremades J, Lorenzo R, Sanchez M, et al. Use of antithrombin III in critical patients.
556 *Intensive care medicine*. 1994;20:577-580.
557 59. Eisele B, Heinrichs H, Delvos U, et al. Antithrombin III in patients with severe sepsis: a
558 randomized, placebo-controlled, double-blind multicenter trial plus a meta-analysis on all
559 randomized, placebo-controlled, double-blind trials with antithrombin III in severe sepsis.
560 *Intensive care medicine*. 1998;24:663-672.
561 60. Baudo F, Caimi T, DeCataldo F, et al. Antithrombin III (ATILL) replacement therapy in
562 patients with sepsis and/or postsurgical complications: a controlled double-blind, randomized,
563 multicenter study. *Intensive care medicine*. 1998;24:336-342.
564 61. Abraham E, Reinhart K, Svoboda P, et al. Assessment of the safety of recombinant tissue
565 factor pathway inhibitor in patients with severe sepsis: a multicenter, randomized, placebo-
566 controlled, single-blind, dose escalation study. *Critical care medicine*. 2001;29(11):2081-2089.
567 62. Abraham E, Reinhart K, Opal S, et al. Efficacy and safety of tifacogin (recombinant tissue
568 factor pathway inhibitor) in severe sepsis: a randomized controlled trial. *Jama*. 2003;290(2):238-
569 247.
570 63. Bernard G. Recombinant human activated protein C worldwide evaluation in severe sepsis
571 (PROWESS) study group: efficacy and safety of recombinant human acitvated protein C for severe
572 sepsis. *N Engl J Med*. 2001;344:699-709.
573 64. Nadel S, Goldstein B, Williams MD, et al. Drotrecogin alfa (activated) in children with
574 severe sepsis: a multicentre phase III randomised controlled trial. *The Lancet*.
575 2007;369(9564):836-843.
576 65. Ranieri VM, Thompson BT, Barie PS, et al. Drotrecogin alfa (activated) in adults with
577 septic shock. *New England Journal of Medicine*. 2012;366(22):2055-2064.
578 66. Wunderink RG, Laterre P-F, Francois B, et al. Recombinant tissue factor pathway inhibitor
579 in severe community-acquired pneumonia: a randomized trial. *American journal of respiratory*
580 *and critical care medicine*. 2011;183(11):1561-1568.
581 67. Feldmann K, Grandoch M, Kohlmorgen C, et al. Decreased M1 macrophage polarization
582 in dabigatran-treated Ldlr-deficient mice: implications for atherosclerosis and adipose tissue
583 inflammation. *Atherosclerosis*. 2019;287:81-88.
584 68. Gorzelak-Pabiś P, Broncel M, Pawlos A, et al. Dabigatran: Its protective effect against
585 endothelial cell damage by oxysterol. *Biomedicine & Pharmacotherapy*. 2022;147:112679.
586 69. Skeik N, Westergard E. Recommendations for VTE prophylaxis in medically ill patients.
587 *Annals of vascular diseases*. 2020;13(1):38-44.

70. Eck RJ, Elling T, Sutton AJ, et al. Anticoagulants for thrombosis prophylaxis in acutely ill patients admitted to hospital: systematic review and network meta-analysis. *bmj*. 2022;378

Mechanism of Action (MoA)	How often MoA occurs among candidate drugs from Table S2
Dopamine receptor antagonist	10
EGFR inhibitor	9
Tubulin inhibitor	8
Adrenergic receptor antagonist	6
MEK inhibitor	6
PI3K inhibitor	6
Serotonin receptor antagonist	6
Calcium channel blocker	5
KIT inhibitor	5
Na/K-ATPase inhibitor	5
RAF inhibitor	5
JAK inhibitor	4
PDGFR inhibitor	4
PKC inhibitor	4
Topoisomerase inhibitor	4

Table 1: MoA of small molecules from Table S2 sorted by the number of times the MoA appears among the list of candidate drugs (only occurrences >= 4 are shown)

Drug Category	Drug identified from current zebrafish LPS screen	Main Mechanism of Action	Drug previously tested with LPS in mammals?/ Novel	Drug previously tested in sepsis?/ Novel
Dopamine and Serotonin Modulators	Ziprasidone	Dopamine and serotonin antagonism	Novel	Novel
	Pergolide	Dopamine receptor agonist	Novel	Novel
	Vilazodone	Inhibits serotonin transporter, partial agonist at serotonin receptors	Novel	Novel
	Brexpiprazole	Dopamine and serotonin receptor modulation	Novel	Novel
	Ketanserin	Serotonin receptor antagonist	Mouse (Liu et al., 2013, Sugino et al., 2009)	Clinical trial for septic shock (Vellinga et al., 2015)
Chemotherapeutics	Rucaparib	Inhibits poly(ADP-ribose) polymerase	Novel	Novel
	Sunitinib	Inhibits receptor tyrosine kinases	Mouse (Zhao et al., 2019)	Novel
	Fedratinib	Inhibits janus receptor kinase 2	Human macrophages (Akcora et al., 2019)	Novel
	Pralsetinib	Rearranged during transfection kinase inhibitor	Novel	Novel
	Ceritinib	Inhibits autophosphorylation of anaplastic lymphoma kinase	Human endothelial cells (Dayang et al., 2021, Hu et al., 2019)	CLP induced sepsis in mice (Hu et al., 2019)
	Amsacrine	DNA intercalator	Novel	Novel
Antiviral/ Antibacterial Agents	Nelfinavir	Protease inhibitor	Human macrophages (Wallet et al., 2012)	CLP induced sepsis in mice (Weaver et al., 2004)
	Saquinavir	Protease inhibitor	Mouse (Yao et al., 2023, Tong et al., 2021), Human lung cells (Zhang et al., 2018)	CLP induced sepsis in mice (Tong et al., 2021)
	Ledipasivir	Inhibits viral phosphorylation	Novel	Novel
	Bedaquiline	Blocks proton pump for ATP synthase	Novel	Novel

653 **Table 2: Small molecules protecting zebrafish embryos from LPS toxicity.**

654

Drug Category	Drug identified from current zebrafish LPS screen	Main Mechanism of Action	Drug previously tested with LPS in mammals?/ Novel	Drug previously tested in sepsis?/ Novel
Miscellaneous	Indacaterol	β-adrenoreceptor agonist	Guinea pigs (Aritake et al., 2021), Human lung macrophages (Maarsingh et al., 2021)	Novel
	Conivaptan	Vasopressin receptor antagonist	Novel	Novel
	Deserpidine	Vesicular monoamine transporter blocker	Novel	Novel
	Lomitapide	Microsomal triglyceride transfer protein inhibitor	Novel	Novel
	Dabigatran	Thrombin inhibitor	Mouse (Kimura et al., 2020)	Mouse sepsis models, including CLP (Lei et al., 2021), *S. aureus* bacteremia in humans (Butt et al., 2021)
	Berberine	Activates AMPK (increases glycolysis)	Mouse (Chen et al., 2022), rats (Chen et al., 2021, Zhao et al., 2023), mouse macrophage cells (Zhao et al., 2023), bovine endometrial epithelial cells (Fu et al., 2023)	CLP-induced sepsis in mice (Chen et al., 2023), cecal slurry-induced sepsis (Li et al., 2021), *S. aureus*-induced septic arthritis in mice (Asila et al., 2022)

655 **Table 2 continued: Small molecules protecting zebrafish embryos from LPS toxicity**

656

657

658

659

660

661 **Figure 1: LPS incubation results in dose-dependent lethality and signs of end-organ damage in**
662 **zebrafish larvae.** (A) Percent survival of 4 days post fertilization (dpf) zebrafish larvae incubated with *S.*
663 *typhi* LPS at 3 dpf. 3 clutches of 15 fish (total of 45) were used per concentration. (B) Heart rate (beats
664 per minute) was counted 3 hours after LPS (40 μg/mL) administration and compared to controls. Each
665 point represents a different fish, and the results include 3 separate experiments. (C) *grk5*, a gene involved
666 in heart rate contractility, was measured by qPCR in LPS-treated fish compared to controls. Larvae from
667 two or more clutches were pooled, where each point represents a separate clutch, and the average fold
668 change in LPS-treated fish vs. controls was graphed. 30-45 total fish were used per time point. Bars
669 indicate mean and standard deviation. Student's t-test (two-tailed) on $\Delta\Delta C_t$ values was used to determine
670 significance. *P<0.05.
671
672 **Figure 2: The immune and interferon signaling pathways and procoagulant pathways are**
673 **significantly upregulated in LPS-treated fish compared to controls.** (A) KEGG pathway analysis of
674 RNA-seq data from whole LPS treated fish compared to controls. Significantly changed genes (adjusted
675 p-value <0.05) from RNA-seq data on pooled 3 dpf LPS-treated vs. control fish (consisting of 30-45
676 embryos per category) performed in triplicate were used for further analyses. These genes were converted
677 to human versions and then submitted for KEGG Pathway Analysis using the Enrichr platform, a publicly
678 available tool developed by the Ma'ayan lab at Icahn School of Mount Sinai, NY (Chen et al., 2013,
679 Kuleshov et al., 2016). Overlap score is the number of significantly changed genes over the total number
680 of genes in the pathway. Combined score considers the z-score (a value's relationship to the mean) in
681 addition to the adjusted p-value. The combined score is used to assess the significance of gene set
682 enrichment findings, with higher values being more significant. Adjusted p-value <0.05 is considered
683 significant. Immune and interferon-related and complement and coagulation pathways are shown. For
684 complete analysis, see Table S1. (B) A subset of genes in the immune and interferon pathways were
685 tested by qPCR, using 3 dpf larvae treated with 40 μg/mL LPS vs. control conditions. Larvae from two or
686 more clutches were pooled, where each point represents a separate clutch, and the average fold change in

687 LPS-treated fish vs. controls is graphed. Bars represent mean and standard deviation. Student's t-test
688 (two-tailed) on $\Delta\Delta C_t$ values was used to determine significance. *P<0.05. (C) A subset of procoagulant
689 genes was tested by qPCR, using 3 dpf larvae treated with 40 μg/mL LPS vs. control conditions. Larvae
690 from two or more clutches were pooled, where each point represents a separate clutch, and the average
691 fold change in LPS-treated fish vs. controls is graphed. Bars indicate mean and standard deviation.
692 Student's t-test (two-tailed) on $\Delta\Delta C_t$ values was used to determine significance. *P<0.05. A schematic of
693 the laser injury assay used to measure time to occlusion is shown in (D), where the time to formation of
694 an occlusive thrombus after laser pulses were delivered to the posterior cardinal vein or dorsal aorta was
695 measured. 120 seconds was the maximum time each larva was observed. Time to occlusion (TTO) after
696 laser injury in the venous (E) and arterial (F) circulation was measured in 3 dpf zebrafish larvae 3 hours
697 after LPS administration and compared to controls. Each point represents a separate fish, and the observer
698 was blinded to the treatment condition. P<0.05 is considered significant by Mann-Whitney *U* testing.
699
700 **Figure 3: The anticoagulant dabigatran mitigates LPS-induced lethality and reduces the expression**
701 **of inflammatory genes.** (A) Zebrafish were administered a lethal dose of LPS with 25 μM dabigatran
702 along with appropriate controls and survival was tracked daily from 3 through 6 dpf. (B) Expression of
703 inflammatory genes was evaluated by qPCR 3 hours after drug administration in 3 dpf larvae treated with
704 LPS and dabigatran. Pooled larvae (15-45) from a clutch were used, where each point represents a
705 separate clutch, and the average fold change in LPS-treated fish vs. controls is graphed. Bars indicate
706 mean and standard deviation. Student's t-test (two-tailed) on $\Delta\Delta C_t$ values was used to determine
707 significance. *P<0.05. (C) Time to occlusion (TTO) after laser injury in the venous circulation was
708 measured in 3 dpf zebrafish larvae 3 hours after LPS and dabigatran administration. Each point represents
709 a single larva, and the observer was blinded to the condition. P<0.05 was considered significant by Mann-
710 Whitney *U* testing.
711

712 **Figure 4: Dabigatran protection from LPS toxicity occurs independently of prothrombin.** (A) Time
713 to occlusion (TTO) after laser injury in the venous circulation was measured in 3 dpf zebrafish larvae 3
714 hours after LPS and argatroban administration. Each point represents a single larva, and the observer was
715 blinded to the condition. P<0.05 was considered significant by Mann-Whitney *U* testing. (B) Zebrafish
716 were treated with argatroban and/or LPS at 3 dpf and observed daily until 6 dpf for survival. (C) Three
717 dpf larvae from *f2* heterozygous incrosses were divided into four groups: untreated controls, 40 µg/mL
718 LPS, 25 µM dabigatran, and LPS/dabigatran. All groups were followed for 3 days for survival. (D)
719 Genotype distribution of surviving larvae.
720
721 **Figure 5: Dabigatran reduces LPS mediated nitric oxide production.**
722 (A) Representative images of 3 dpf fish stained with DAF-FM DA to visualize nitric oxide production
723 after the indicated treatment. (B) ImageJ analysis showing mean fluorescence intensity of images of 3 dpf
724 DAF-FM DA stained fish with the indicated treatment; observers were blinded to condition. Each point
725 represents a different fish, and the results include 3 separate experiments. Student's t-test (two-tailed) on
726 $\Delta\Delta C_t$ values was used to determine significance. *P<0.05.
727
728 **Figure 6: Dabigatran reduces LPS mediated cell death and apoptosis.**
729 (A) KEGG pathway analysis of RNA-seq data from whole LPS treated fish compared to controls.
730 Significantly changed genes (adjusted p-value <0.05) from RNA-seq data on pooled 3 dpf LPS-treated vs.
731 control fish (consisting of 30-45 embryos per category) performed in triplicate were used for further
732 analyses. These genes were converted to human versions and then submitted for KEGG Pathway Analysis
733 using the Enrichr platform, a publicly available tool developed by the Ma'ayan lab at Icahn School of
734 Mount Sinai, NY (Chen et al., 2013, Kuleshov et al., 2016). Overlap score is the number of significantly
735 changed genes over the total number of genes in the pathway. Combined score considers the z-score (a
736 value's relationship to the mean) in addition to the adjusted p-value. The combined score is used to assess
737 the significance of gene set enrichment findings, with higher values being more significant. Adjusted p-

738 value <0.05 is considered significant. Apoptosis related pathways are shown. For complete analysis, see
739 Table S1. (B) Representative images of 3 dpf fish stained with acridine orange after the indicated
740 treatment. (C) ImageJ analysis showing mean fluorescence intensity of images of 3 dpf acridine orange
741 stained fish with the indicated treatment; observers were blinded to condition. Each point represents a
742 different fish, and the results include 3 separate experiments. Student's t-test (two-tailed) on $\Delta\Delta C_t$ values
743 was used to determine significance. *P<0.05. (D) Representative images of 3 dpf fish stained with
744 TUNEL after the indicated treatment. (E) Apoptosis was scored in 3 dpf TUNEL stained fish with the
745 indicated treatement; observers were blinded to condition. Each point represents a different fish, and the
746 results include at least 2 separate experiments. Student's t-test (two-tailed) on $\Delta\Delta C_t$ values was used to
747 determine significance. *P<0.05.
748
749
750
751
752
753
754
755
756
757
758
759
760
761
762
763

Figure 1

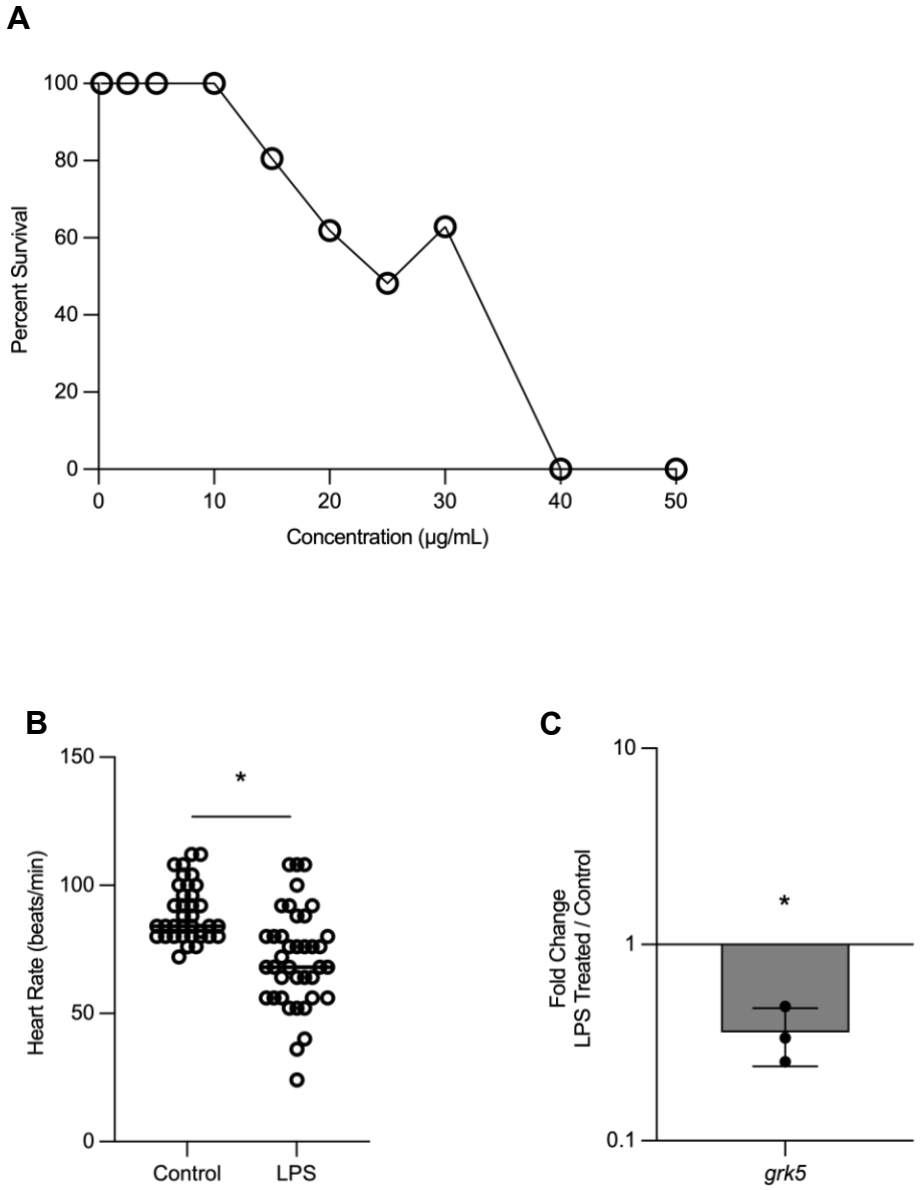
A
Percent Survival
100
80
60
40
20
0
0
10
20
30
40
50
Concentration (µg/mL)
B
Heart Rate (beats/min)
150
100
50
0
*
Control
LPS
C
Fold Change
LPS Treated / Control
10
1
0.1
*
grk5

Figure 2

A

Name of Pathway	**Overall Ranking** (out of 98 significantly changed pathways)	Overlap Score	Adjusted P-value	Combined Score
Pathogenic *E.coli* Infection	1	38/197	2.59E-10	127.749924
Leukocyte Transendothelial Migration	9	21/114	8.13E-06	65.1873171
Complement and Coagulation Cascades	8	18/85	7.42E-06	78.4936729
TNF Signaling	12	20/112	1.84E-05	57.8681584
Platelet Activation	70	14/124	0.017	13.16661224

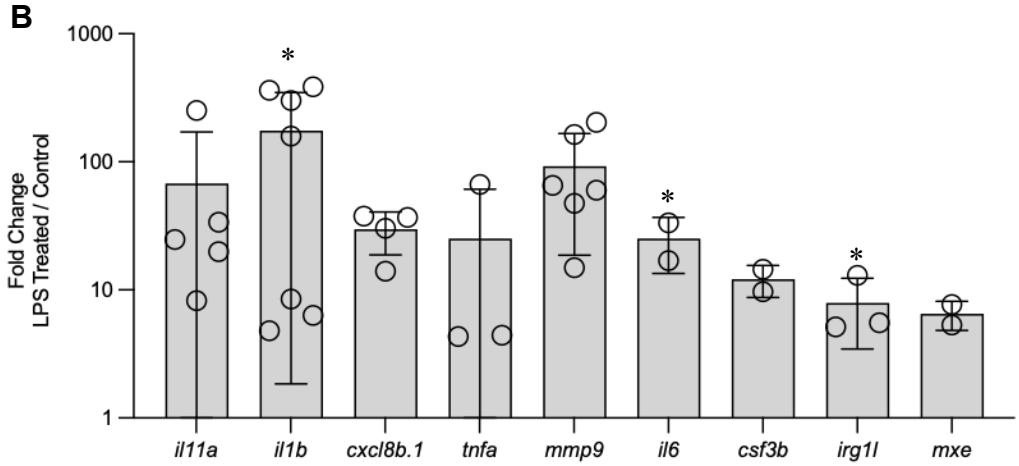

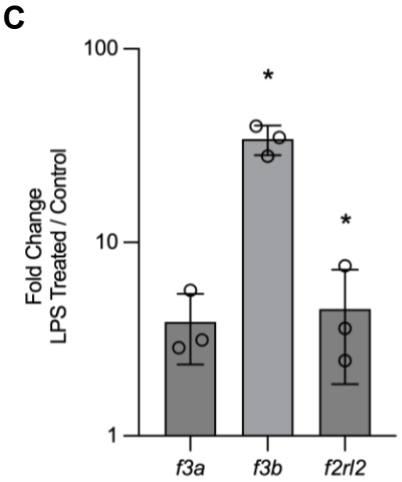

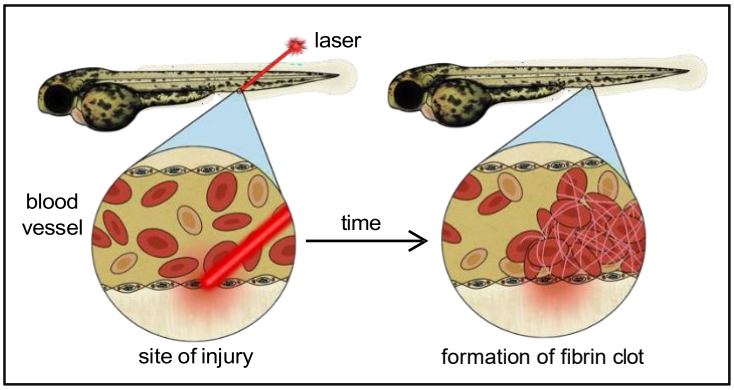

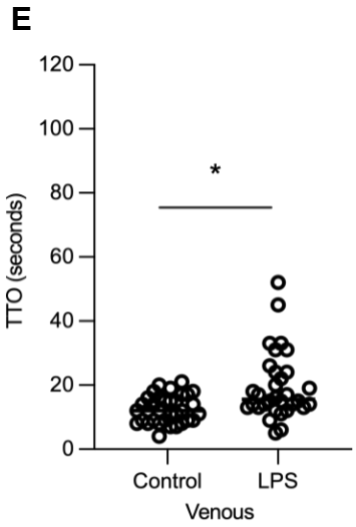

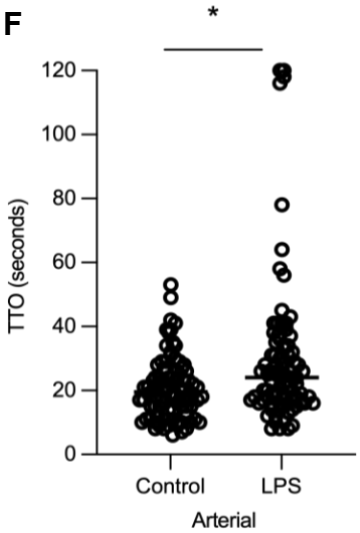

Figure 3

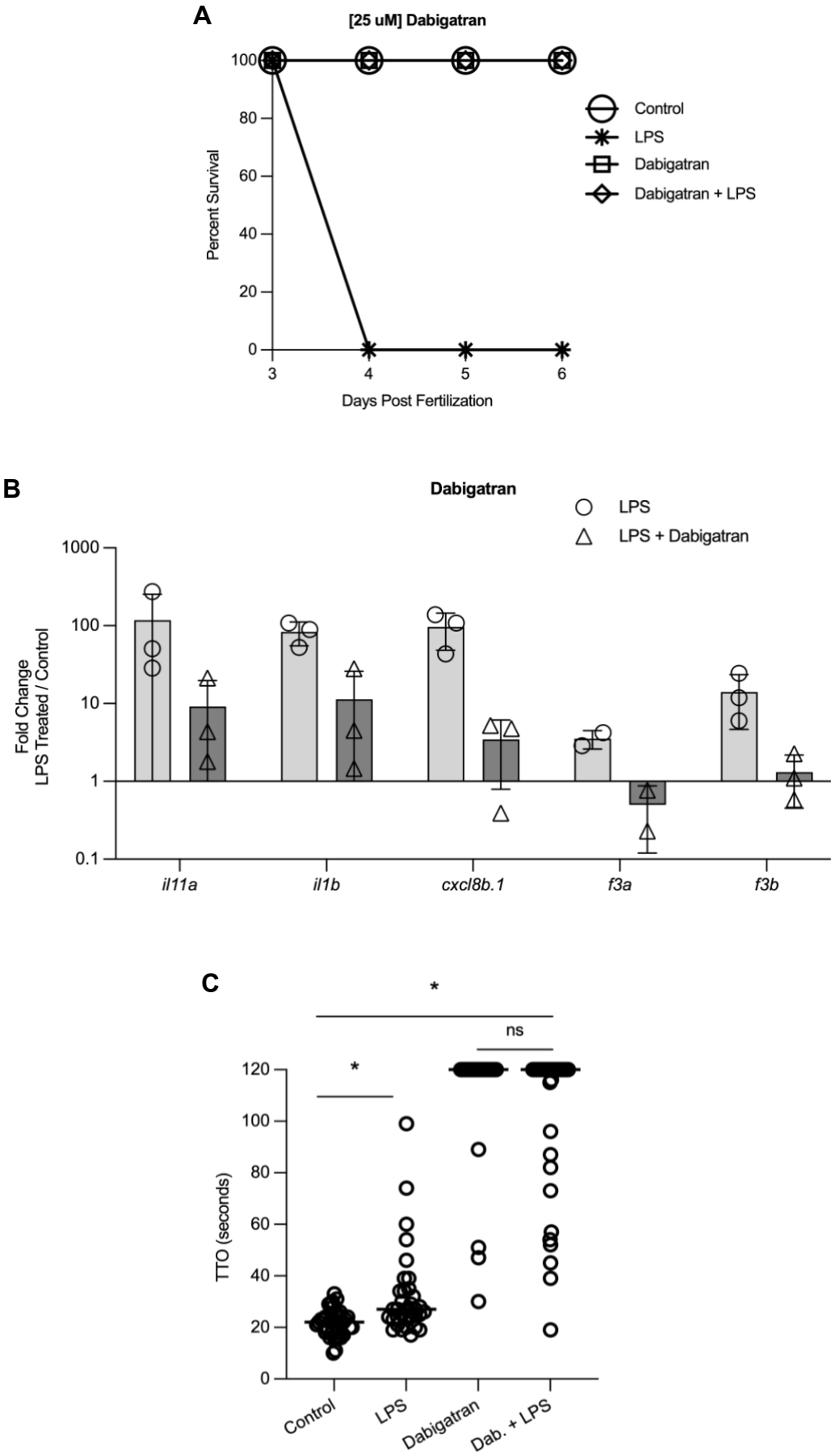
A
[25 uM] Dabigatran
Percent Survival
Days Post Fertilization
Control
LPS
Dabigatran
Dabigatran + LPS
B
Dabigatran
LPS
LPS + Dabigatran
Fold Change
LPS Treated / Control
il11a
il1b
cxcl8b.1
f3a
f3b
C
TTO (seconds)
ns
Control
LPS
Dabigatran
Dab. + LPS

Figure 4

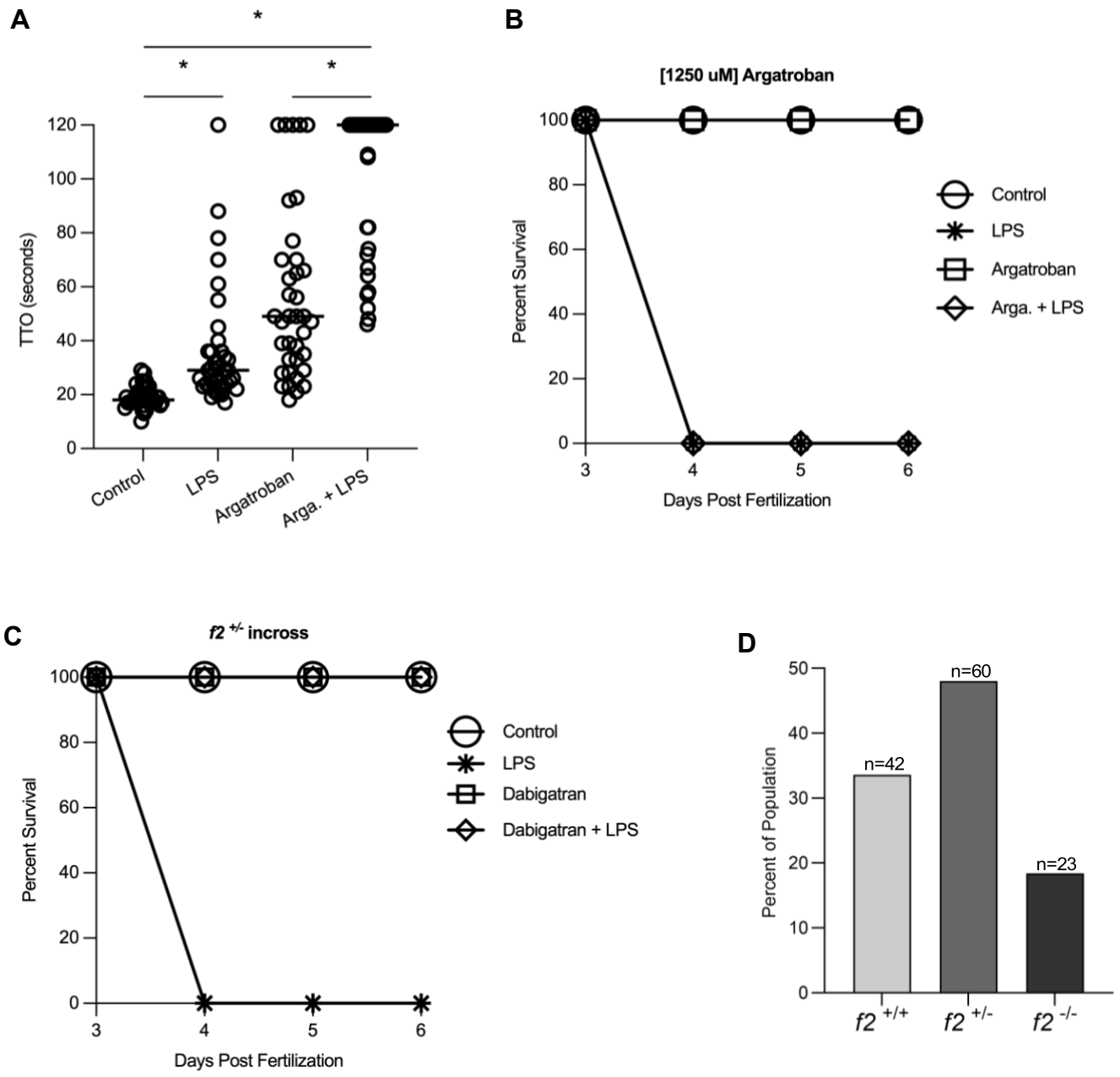
A
*
*
*
TTO (seconds)
120
100
80
60
40
20
0
Control
LPS
Argatroban
Arga. + LPS
B
[1250 uM] Argatroban
Percent Survival
100
80
60
40
20
0
3
4
5
6
Days Post Fertilization
Control
LPS
Argatroban
Arga. + LPS
C
f2 +/- incross
Percent Survival
100
80
60
40
20
0
3
4
5
6
Days Post Fertilization
Control
LPS
Dabigatran
Dabigatran + LPS
D
Percent of Population
50
40
30
20
10
0
n=42
n=60
n=23
f2 +/+
f2 +/-
f2 -/-

Figure 5

A

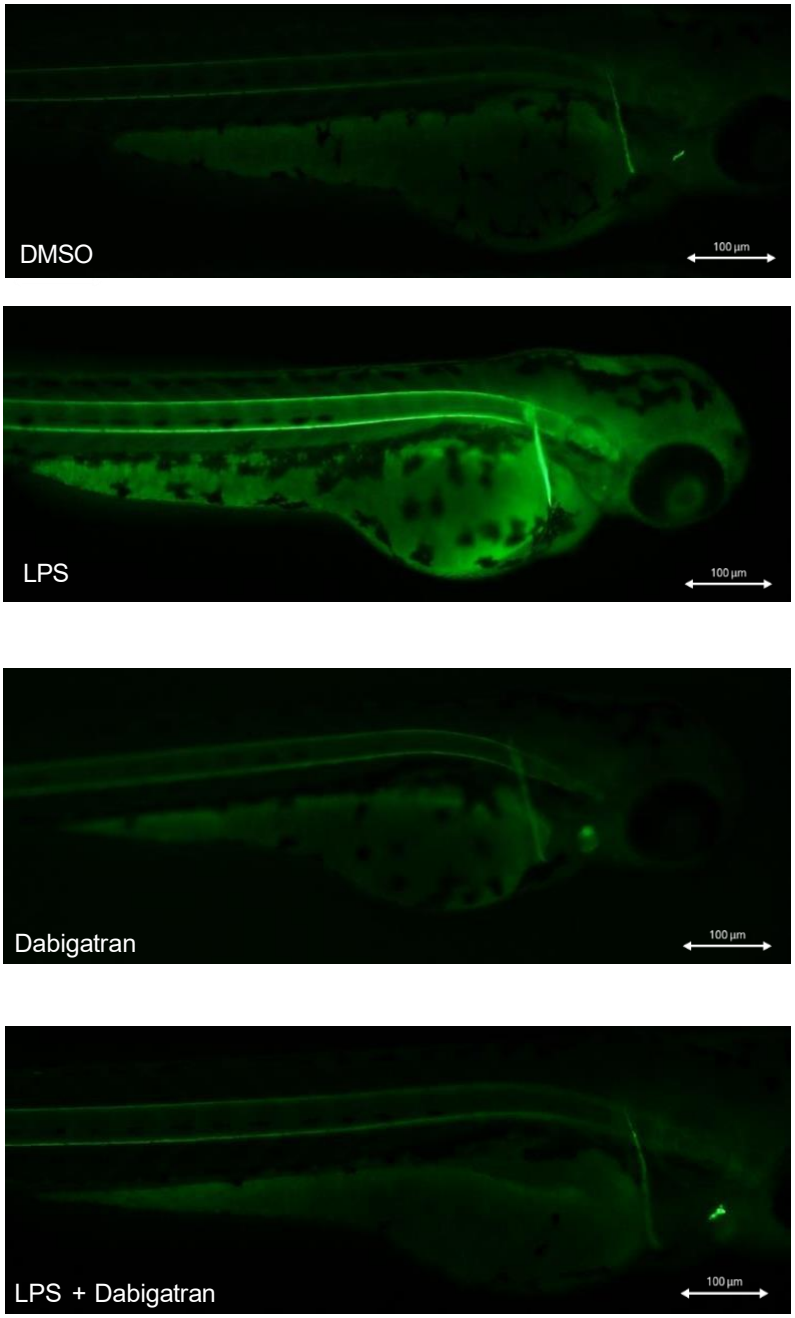
DMSO
100 µm
LPS
100 µm
Dabigatran
100 µm
LPS + Dabigatran
100 µm

B

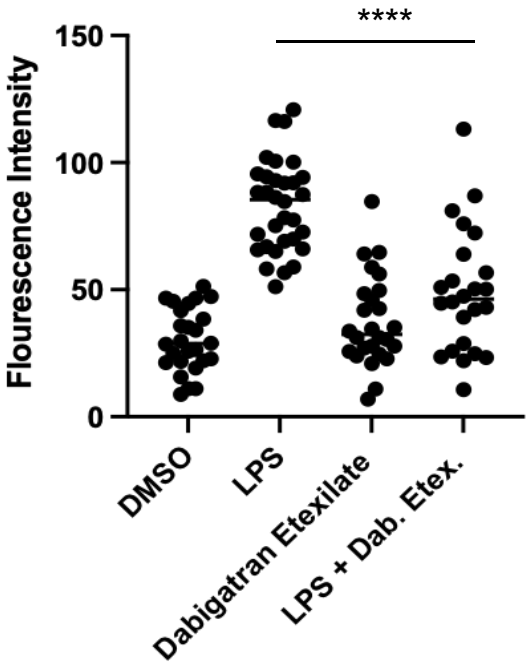
****
Flourescence Intensity
150
100
50
0
DMSO
LPS
Dabigatran Etexilate
LPS + Dab. Etex.

Figure 6

A

Name of Pathway	Overall Ranking (out of 98 significantly changed pathways)	Overlap Score	Adjusted P-value	Combined Score
Apoptosis	11	23/142	1.84 E-05	51.783249

B

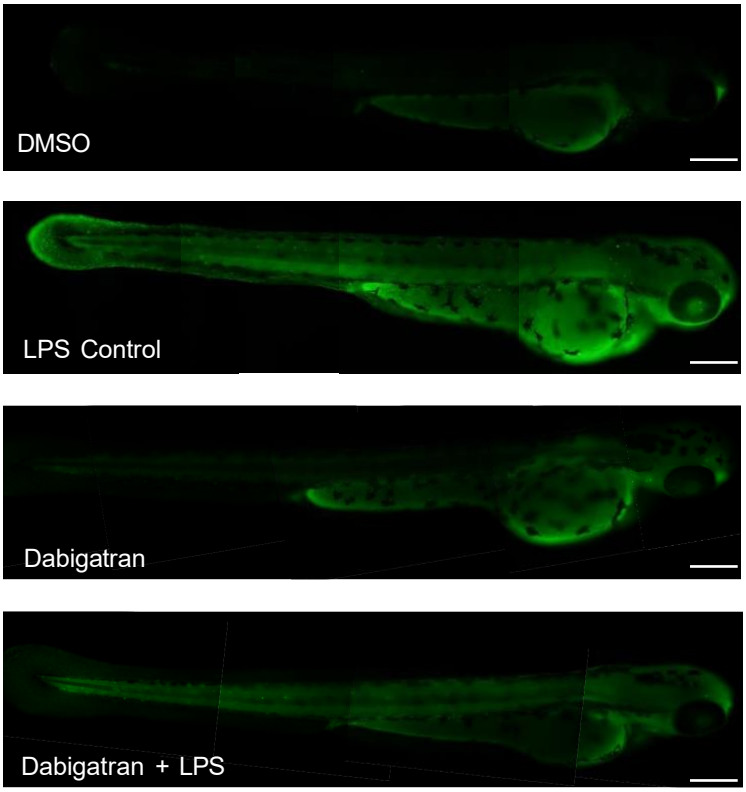

C

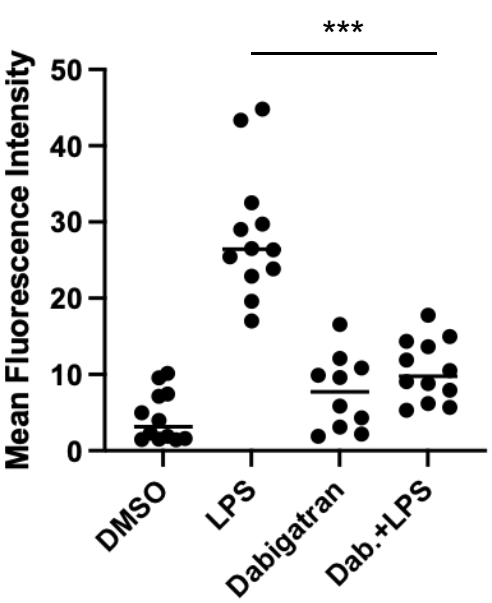

D

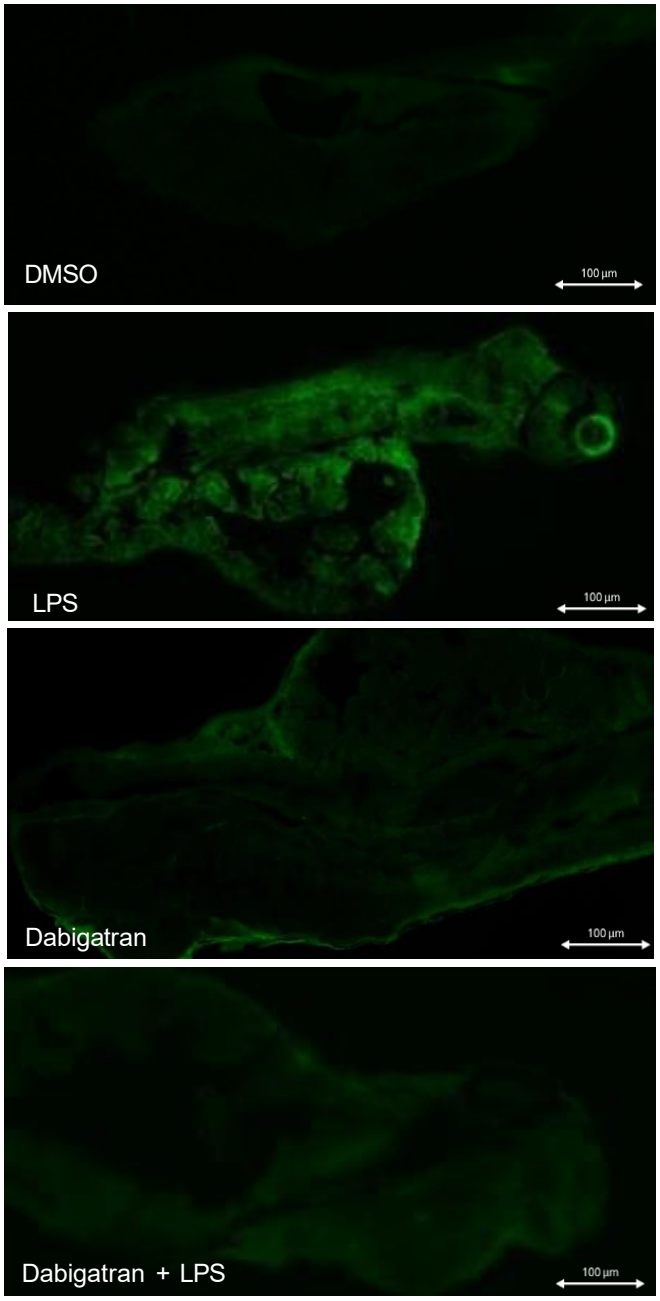
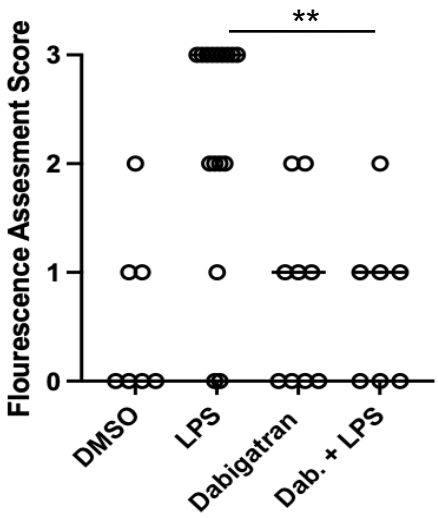
E